



Vascular apoptosis associated with meglumine antimoniate: *In vivo* investigation of a chick embryo model

Ahmad Khosravi ^a, Iraj Sharifi ^{a,*}, Hadi Tavakkoli ^{b,**}, Ali Reza Keyhani ^a, Ali Afgar ^c, Zohreh Salari ^d, Seyedeh Saedeh Mosallanejad ^a, Mehdi Bamorovat ^a, Fatemeh Sharifi ^a, Saeid Hassanzadeh ^b, Balal Sadeghi ^e, Shahriar Dabiri ^f, Abbas Mortazaeizadeh ^f, Zahra Sheikhshoae ^f, Ehsan Salarkia ^a

^a Leishmaniasis Research Center, Kerman University of Medical Sciences, Kerman, Iran

^b Department of Clinical Science, School of Veterinary Medicine, Shahid Bahonar University of Kerman, Kerman, Iran

^c Research Center for Hydatid Disease in Iran, Kerman University of Medical Sciences, Kerman, Iran

^d Obstetrics & Gynecology Center, Afzalipour School of Medicine, Kerman University of Medical Sciences, Kerman, Iran

^e Food Hygiene and Public Health Department, Faculty of Veterinary Medicine, Shahid Bahonar University of Kerman, Kerman, Iran

^f Afzalipour School of Medicine & Pathology and Stem Cells Research Center, Kerman University of Medical Sciences, Kerman, Iran

ARTICLE INFO

Article history:

Received 25 August 2018

Accepted 22 September 2018

Available online 5 October 2018

Keywords:

Apoptosis

Chick embryo

Meglumine antimoniate

Leishmaniasis

Toxicity

ABSTRACT

The vasculo-toxic effect of meglumine antimoniate (MA) was confirmed in our previous investigation. The current study investigates the association of this effect with altered VEGF-A and VEGF-R2 expression. Additional mechanisms by which MA causes vascular toxicity are not clearly understood. We hypothesized that MA may alter normal expression of apoptotic genes and cause vascular toxicity. The current investigation was designed to address this issue using a chick embryo model. Fertile chicken eggs were treated with MA and the extra-embryonic membrane (EEM) vasculature was evaluated by morphometric, molecular and immunohistochemistry assays. The results showed that MA not only altered apoptotic gene expression, but that this alteration may disturb the normal development of the vascular network and cause embryo malformation. The relative expression level of the CASP3, CASP7, CASP9, APAF1, AIF1 and TP53 genes increased in drug-exposed EEMs. In addition, IHC assay confirmed the low expression BCL2 and increased expression of Bax, which are associated with a high rate of apoptosis. We suggest that induction of an apoptotic signaling pathway can lead to vascular defects during embryo development and the consecutive cascade of events can lead to the embryo malformation.

© 2018 Elsevier Inc. All rights reserved.

1. Introduction

The normal intra-uterine growth of a fetus is associated with the normal development of the vascular network. Consuming prescription drugs during pregnancy may alter embryo growth and vascular development and induce malformations [1–4]. It is important to consider that the genesis, proliferation and regression

of the vascular network are associated with different pathways and factors. One of the most important is the normal expression of apoptotic-regulating genes such as caspase family proteins (CASP), apoptotic protease activating factor (APAF), apoptosis-inducing factor (AIF) and tumor protein p53 (TP53).

At the present time, leishmaniasis is an important parasitic disease worldwide and accounts for over 58,000 deaths per annum [5]. Meglumine antimoniate (MA), a carbohydrate-antimony oligomer, is the first-line regime for treatment of leishmaniasis. Because drug toxicity is of great concern during pregnancy, we showed that MA was able to induce vascular toxicity in the chick extra-embryonic membrane (EEM) and that the use of MA during pregnancy should be considered as potentially embryo-toxic [6]. In that study, chick embryos and EEMs were used as a preclinical model applicable to the evaluation of the toxic effects of drugs

* Corresponding author. Leishmaniasis Research Center, Kerman University of Medical Sciences, 22 Bahman Boulevard, Pajouhesh Square, Postal Code: 76169-14115, Kerman, Iran.

** Corresponding author. School of Veterinary Medicine, Shahid Bahonar University of Kerman, Iran.

E-mail addresses: iraj.sharifi@yahoo.com (I. Sharifi), tavakkoli@uk.ac.ir (H. Tavakkoli).

Abbreviations

AIF	Apoptosis-inducing factor
APAF	Apoptotic protease activating factor
CASP	Caspase family proteins
CI	Confidence interval
EEM	Extra-embryonic membrane
GAPDH	Glyceraldehyde-3-phosphate dehydrogenase
HH	Hamburger and Hamilton
MA	Meglumine antimoniate
TP53	Tumor protein p53
IHC	Immunohistochemistry
H&E	Haematoxylin and eosin
HPRT	Hypoxanthine Phosphoribosyltransferase

[7–10]. They are also used to investigate the effects of drugs on pathways associated with vessel genesis and regression [11–13].

Various mechanisms and pathways are associated with the vasculo-toxic properties of MA. We have investigated whether or not MA alters the expression of VEGF-A and its receptor in the extra-embryonic vascular plexus [6]. Additional pathways by which MA affects vascular toxicity are not yet clearly understood. One of the most important factors that influences the normal development of vascular network is apoptosis. We hypothesize that MA may alter apoptotic gene expression and cause vascular toxicity. This phenomenon has not been evaluated in the literature thus far; therefore, the current investigation was designed to address the following questions:

- I. Does MA cause *in vivo* vascular apoptosis?
- II. Does MA alter expression of molecular pathways associated with vascular apoptosis?
- III. Does the induction of vascular apoptosis cause embryo malformation?

A chick embryo model was applied to address these questions. Specialized software was used to analyze the vascular pattern in chick EEMs in order to determine possible MA-induced apoptotic activity. The results were enriched with quantitative real-time PCR and immunohistochemistry to assess the effect of the drug on molecular pathways, which is associated with vascular apoptosis. Gross evaluation of the embryo was also done to evaluate the outcome of the induced vascular apoptosis on early embryo formation.

2. Materials and methods

2.1. Effect of MA on vascular apoptosis

To determine the effect of MA on vascular apoptosis, the EEM vasculature was evaluated by morphometric, molecular and immunohistochemistry assays as described below.

2.2. Drug

Meglumine antimoniate (Glucantime) injectable solution was obtained from Sanofi-Aventis, Pharmaceuticals (France). Each milliliter of the drug contains 300 mg MA. Various dosages of MA (75 and 150 mg/per kg of egg weight, which are equal to and higher than the therapeutic dosages used in humans, respectively) were used to evaluate the effect of the drug on vascular apoptosis [6].

2.3. Eggs

Fertilized chicken eggs (Ross 308, *Gallus gallus*) were obtained from Mahan Breeder (Iran). The eggs were incubated at 37.5 °C and 60% relative humidity.

2.4. Application of the drug

The experiment was performed according to European ethical guidelines for the care of animals in experimental investigations and in line with the guidelines of Kerman University of Medical Sciences. It was approved by the Animal Ethics Committee of the Research Council of Kerman University of Medical Sciences in Iran (project no. 94/974/205; ethics no. IR.KMU.REC.1394.525).

The embryonated eggs were divided into three treatment groups containing 10 eggs each. In Group 1 (control group), the embryonated eggs were injected with sterile phosphate buffered saline (PBS) at 50 µl/egg. The eggs of groups 2 and 3 were likewise treated with MA at dosages of 75 or 150 mg/egg, respectively. MA or sterile PBS was injected after 24, 48 and 72 h of the incubation period (to developmental stages 6, 12 and 20 h, respectively).

The staging of the embryos was performed according to the Hamburger and Hamilton (HH) method [14]. A pinpoint hole of approximately 0.5 mm was made in the eggshell and the outer shell membrane at the blunt end of the egg and the embryo received treatment by direct injection into the inner shell membrane using a 50 µl Hamilton syringe. This method of injection has been described elsewhere [15,16]. Following administration of the drugs, the hole was sealed with warmed paraffin (Merck; Germany) and the embryos were allowed to develop for a further day. On day 4 of incubation, a window of 25 mm by 25 mm was made in the eggshell to allow for visualization of the EEM vasculature.

2.5. Imaging

High-quality images (resolution of 4000 × 3000 pixels) were captured by a stereomicroscope (Luxeo 4D stereozoom microscope; Labomed; USA) attached to a Canon EOS 700D camera supported by Luxeo software. Images were acquired from the EEMs of the embryos and their vasculature. The microscopic images were captured at 10 × magnification.

2.6. Morphometric analysis of vascular plexus

Digimizer4.3.0 (MedCalc; Belgium), ImageJ 1.48 (National Institutes of Health; USA) and MATLAB (Mathworks; Matlab R2015a) were used for quantification of the vascular plexus. Briefly, the captured images of the chick EEM were loaded into the software and the area of interest (2800 × 3000 pixels) was extracted from the images in TIFF format. One-half of the vascular bed (right lateral vitelline plexus) was selected for analysis. This area was uniform in all images and was located at the right side of the anterior vitelline vein and the posterior vitelline vein (Fig. 1A, B and C). The threshold of the images was improved to optimize edge detection and converted to a binary format. This method applies a different color value to each pixel and determines the vasculature and the nonvascular areas in the images. Finally, the images are skeletonized.

2.7. Measurements

The percentage of the area of the vessels and total vessel length (mm) were determined for the selected vascular bed. To assess the effect of MA on the pattern of the vascular plexus, the vessels were assigned to subgroups according to their diameters. The vessels

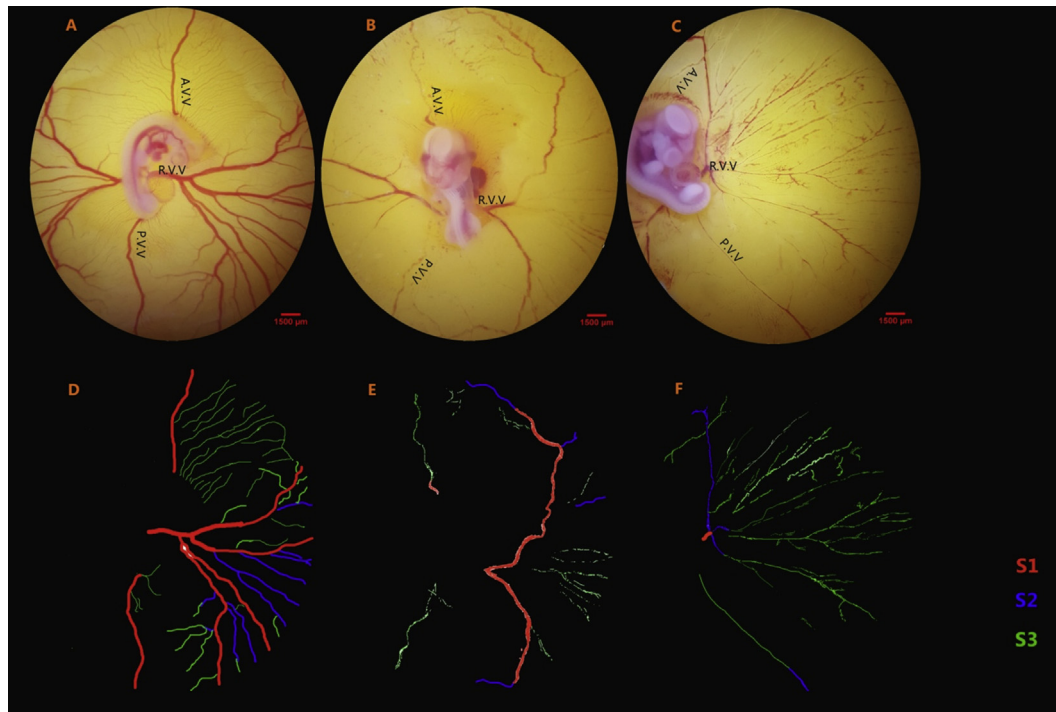


Fig. 1. Extra-embryonic membrane vasculatures of the day 4 chicken embryos are presented to illustrate the image manipulations required for analysis of vascular plexus. The images are acquired from the embryo of the control (A and D) and meglumine antimoniate at dosages of 75 (B and E) or 150 (C and F) mg/kg egg-weight. (A, B and C) areas of interest (2800 × 3000 pixels) are extracted from the captured images. (D, E and F) the R.V.V. that is located at the right sides of the A.V.V. and P.V.V. was selected for analysis. S1, the vessels by the largest diameter, until S3, the vessels by the smallest diameter. A.V.V., anterior vitelline vein; P.V.V., posterior vitelline vein; R.V.V., right lateral vitelline plexus.

with the largest diameters ($\geq 25 \mu\text{m}$) were classified as subgroup 1 (S1). The vessels of subgroup 2 (S2) had diameters that were 71% of the S1 diameter and S3 had diameters that were 71% of the S2 diameter (Fig. 1D, E and F). This method of classification was based on the fact that, when a blood vessel branches, blood flows most efficiently is 71% of the main branch [17].

2.8. Effect of MA on expression of vascular apoptosis

Quantitative real-time PCR (qPCR) was done to assess the effect of MA on the expression of genes that are associated with vascular apoptosis. First, the EEMs were dissected from embryos and the relative expression levels of the CASP3, CASP7, CASP9, APAF1, AIF1 and TP53 genes were determined by qPCR. The total RNA of the extra-embryonic membrane was isolated using a RNeasy mini kit (Qiagen; USA). The cDNA was synthesized using a total of 500 ng RNA and a RT reagent kit (Takara; Clontech) according to protocol. Quantitative real-time PCR was performed using a SYBR Green assay (SYBR Premix Ex Ta II; Japan). The specific primers and reference gene sequences are listed in Table 1. Expression levels were calculated relative to the expression levels of the selected

reference gene (GAPDH and HPRT).

In the next step, STRING v10.5 (<http://string.embl.de/>) was used to construct a protein-protein interaction network of the genes in this study. Here, the network is constructed using active interaction sources such as text mining, high-throughput experiments, co-expression and previous knowledge of databases.

2.9. Histopathological evaluation

The tissues samples of 30 chick embryos were selected and fixed in 10% buffered formalin and were embedded in paraffin. Five μm thick tissue sections were cut by the microtome (Slee-Germany) from the block paraffin and samples were stained with the haematoxylin and eosin (H&E) for histopathological study. Afterward the immunohistochemical (IHC) staining was performed for Bcl2 (mouse monoclonal antibody, American, code number: PDMO16-lotH147) and Bax (Zytomed_Germany, code number: 502_17990) markers. The expression of Bcl2 and Bax were measured by counting the positively stained cells and considering the mean in 10 high-power fields (400 \times), (Fig. 2b).

Table 1
The designed primers and standard gene sequences for quantitative real-time PCR.

Gene (Gallus gallus)	Forward sequence (5'–3')	Reverse sequence (5'–3')	Product size (bp)
Casp3	TGCCCTCTTGAAGTCAAAG	TCCACTGTCTGCTTCAATACC	139
Casp7	AGGCTCTGGTTGTGCAGT	CGCAAGGAATCTGCTTCTTC	161
Casp9	GTCAGACATCGTATCCACCAAGG	ACAGCCAGCCAGACCAGGAACACC	198
APAF1	TTGCCAACCAGAGACATCAGAGG	TGCCGACGAACAACAACCAGACG	128
AIF1	GCGTTAATGTTTATATGCCTAATG	CCTCCGAAGTCAGAATCC	181
TP53	ACCTGCACCTTACTCCCGGT	TCTTATAGACGGCCACGGCG	127
HPRT	GATGAACAAGGTTACGACTCGGA	TATAGCCACCCTTGAGTACACAGAG	103
GAPDH	CCTCTCTGGCAAAGTCCAAG	GGTACGCTCTCGGAAGATA	176

2.10. Effect of MA on early embryo formation

Following MA treatment, the embryos were examined to assess the outcome of the induced vascular apoptosis on early embryo formation. On day 4 of the incubation period, the eggs were opened at the blunt end and embryos were evaluated under the stereomicroscope to determine any gross abnormalities on the external body surface.

2.11. Statistical analyses

Data were analyzed by GraphPad Prism 6 software. The comparisons between the groups were performed by one-way ANOVA and *t*-test. The mean $2^{-\Delta\Delta ct}$ for treatment and the mean $2^{-\Delta\Delta ct}$ for control for each gene were compared. A difference in the mean values was considered significant at $p < 0.05$.

3. Results

3.1. Effect of MA on vascular apoptosis

We hypothesize that if MA possesses a vascular apoptotic effect, then it alters normal development of the vascular bed; therefore, the EEM vasculatures of the treated embryos were quantified. At the time of imaging (day 4 of incubation), the embryo developmental stage was 22–24 HH. In the control group, a normal blood vessel system surrounded the embryo (Fig. 2AI). The blood circulated in the network of the vascular plexus and directly entered the

vitelline veins or the sinus terminalis and from the sinus terminalis to the vitelline veins. Finally, the vitelline emptied into the omphalomesenteric veins. In the MA-treated embryos, a disturbing pattern of the EEM-vasculature was observed (Fig. 2AII). In severe cases, this was also associated with disseminated intravascular coagulation (Fig. 2AIII). In order to confirm apoptosis in EEM-vasculature, H&E and IHC staining were applied to detect apoptotic cells and its components (Fig. 2B).

3.2. Quantification of vascular plexus

The data acquired from the analysis of the EEM vasculatures are listed in Table 2. Vessel area and total vessel length are presented in percentages and millimeters, respectively. The MA-treated embryos showed a reduction in vascular parameters compared to the control embryos. The vessel area and total vessel length were significantly lower in MA-treated embryos compared to control. A greater decrease was associated with embryos that received the highest dosage of the drug ($p = 0.018$).

3.3. Pattern of vascular plexus

To assess the pattern of the vascular plexus after MA treatment, the vessels of the EEM were assigned to subgroups according to diameter size with S1 having vessels of the largest diameter and S3 the smallest diameter (Fig. 1D, E and F). As shown in Table 2, MA significantly reduced the total vessel length of the S1, S2 and S3 subgroups ($p < 0.05$).

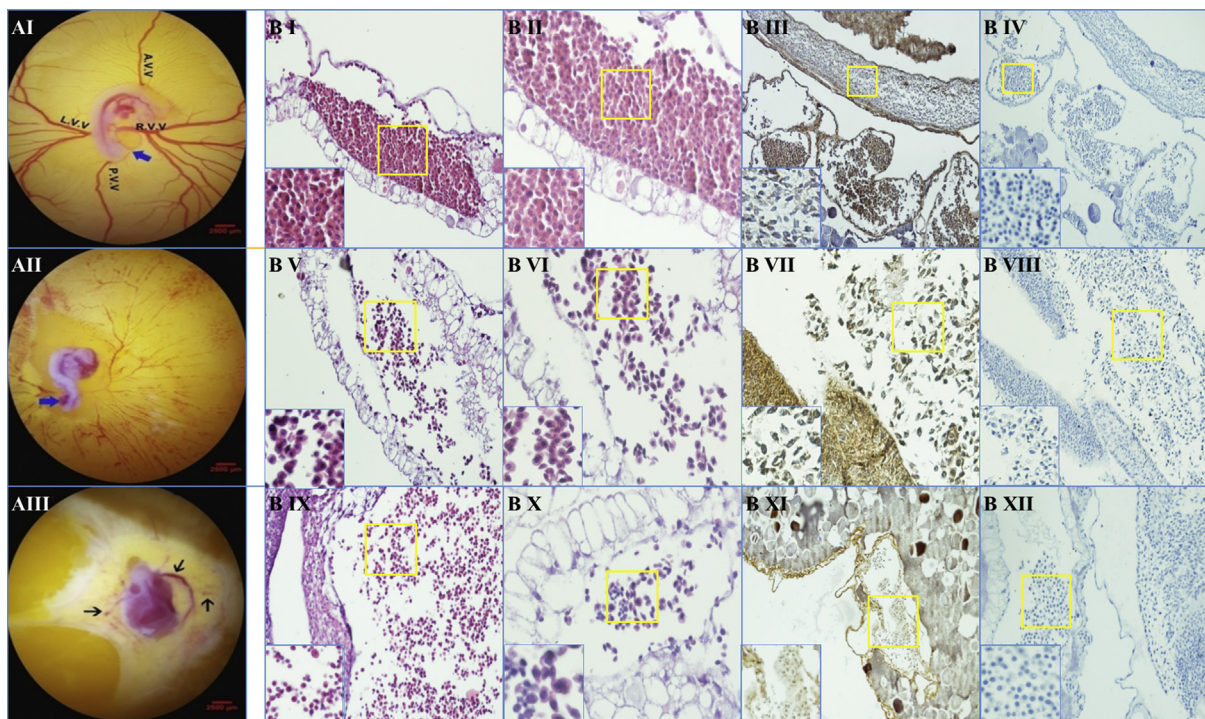


Fig. 2. Meglumine antimoniate possesses vascular apoptotic effect and affects blood vessel system. **A.** The chick's extra-embryonic membrane was (AI) untreated or (AII and AIII) treated with 75 or 150 mg/kg egg-weight of meglumine antimoniate, respectively. (AI) Control embryo with normal blood vessel system and normal C-shape is seen. Lower limbs and tail tip grow ventrally in the same direction (blue arrow). (AII) Blood vessel system is disrupted. Twisting in the lumbosacral region of the body makes the embryo S-shape at the craniocaudal axis. Lower limbs grow dorsally to the tail tip (blue arrow). (AIII) The abnormal embryo is seen; arrows show disseminated intravascular coagulation. A.V.V., anterior vitelline vein; L.V.V., left lateral vitelline vessel; P.V.V., posterior vitelline vein; R.V.V., right lateral vitelline vessel. **B.** (B I–B IV) Control group, B I (Normal blood vessels filling by mature RBCs and leukocytes (X10), B II (High power view of the same slide (X20), B III and B IV (IHC Staining For Bax and Bcl2); confirmed H&E findings. (B V–B VIII) Meglumine antimoniate-treated embryos at dosages of 75 mg/kg. B V (Dilated vessels filling normal nucleated RBCs and leukocytes), along with few apoptotic cells, (X10) H&E, B VI (High power view (X20) of the same slide), B VII and B VIII (IHC staining for Bax and Bcl2 confirmed H&E findings 75 mg/kg). B IX–B XII Meglumine antimoniate-treated embryos at dosages of 150 mg/kg. B IX (Dilated vessels filling by mature RBCs and leukocytes, along with apoptotic cells (X10) H&E, B X (High power view (X20) of the same slide. B XI–B XII (IHC staining for Bax and Bcl2 confirmed H&E Findings). (For interpretation of the references to color in this figure legend, the reader is referred to the Web version of this article.)

Table 2

Data acquired from vascular analysis of control and MA-treated embryos.

	Control	Meglumine antimoniate	
		75 mg	150 mg
Vessels percentage area	30.32 ± 1.28	13.37 ± 1.75 ^a	7.74 ± 0.88 ^a
Total vessels length (mm)	839.24 ± 35.39	493.82 ± 19.52 ^a	374.18 ± 13.15 ^a
Total vessels length S1 (mm)	218.08 ± 13.09	141.30 ± 7.07 ^a	18.06 ± 3.41 ^a
Total vessels length S2 (mm)	179.1 ± 10.08	105.62 ± 8.80 ^a	53.02 ± 10.36 ^a
Total vessels length S3 (mm)	442.06 ± 10.05	251.09 ± 37.96 ^a	303.10 ± 35.50 ^a

S1, the extra-embryonic membrane vasculature of the largest diameter, until S3, the smallest diameter (data are mean ± SEM, one-way ANOVA).

^a MA treated embryos are significantly different from control embryos.

3.4. Effect of MA on gene expression

The effect of MA on the expression of the genes that are associated with vascular apoptosis is shown in Fig. 3. The mRNA expression levels of CASP3, CASP7, CASP9, APAF1, AIF1 and TP53 genes increased in the MA-treated groups at dosages of 75 or 150 mg/kg of egg weight compared to the control. Statistical analysis revealed that the embryos that received larger volumes of the drug exhibited an increase in gene expression levels in a dose-dependent manner. We also constructed a protein-protein interaction network for the evaluated genes using STRING. Fig. 4A shows the regulated protein-protein network of MA-exposed embryos.

3.5. Embryo malformation

Gross abnormalities were noticed in some embryos, including

disturbing vasculature, especially those treated with 150 mg/kg of egg-weight of MA. The affected embryos had to twist in the lumbosacral region of the body which made them S-shaped at the craniocaudal axis (Fig. 2AII). The control embryos showed a normal C-shape of the longitudinal body axis (Fig. 2A). In addition, in the affected embryos, the lower limbs grew dorsally to the tail tip, whereas in the normal (control) position, the lower limbs and tail tip grew ventrally in the same direction (Fig. 2AI and AII). In severe conditions, especially for those receiving 150 mg/kg of egg-weight of MA, the embryo was thoroughly deformed (Fig. 2AIII).

4. Discussion

Different mechanisms and pathways may be related to the vaso-toxicity of MA. In the current research, details about the vascular apoptotic effect of MA was investigated by employing an

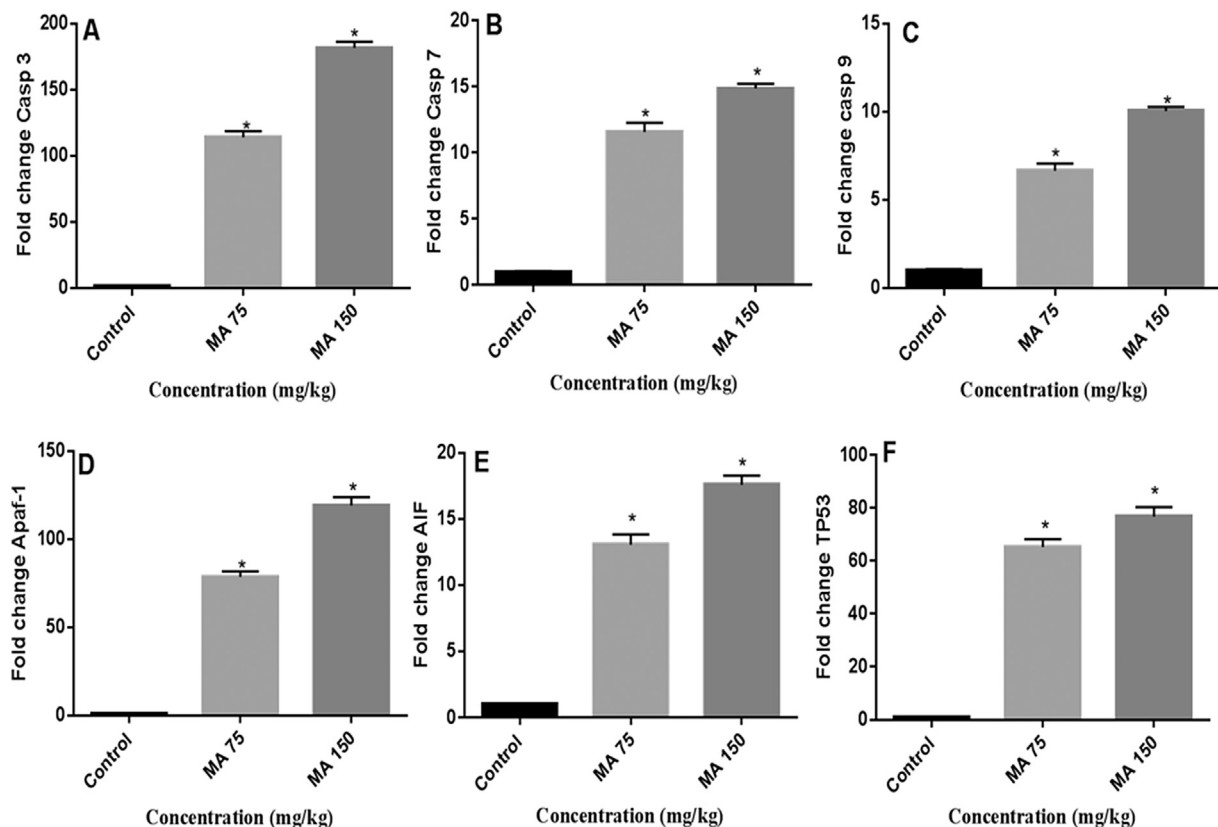


Fig. 3. Meglumine antimonite induced expression of apoptotic mediator genes in the chick's extra-embryonic membrane vasculature. The expression level of (A) CASP3, (B) CASP7, (C) CASP9, (D) APAF1, (E) AIF1 and (F) TP53 genes was increased in the meglumine antimoniate-treated embryos compared to controls. Meglumine antimoniate was administered at dosages of 75 or 150 mg/kg egg-weight. The expression levels were normalized to those of GAPDH and calibrated to controls (data are presented as fold-change value; error bars show standard error of mean; *p < 0.05, One-Way ANOVA).

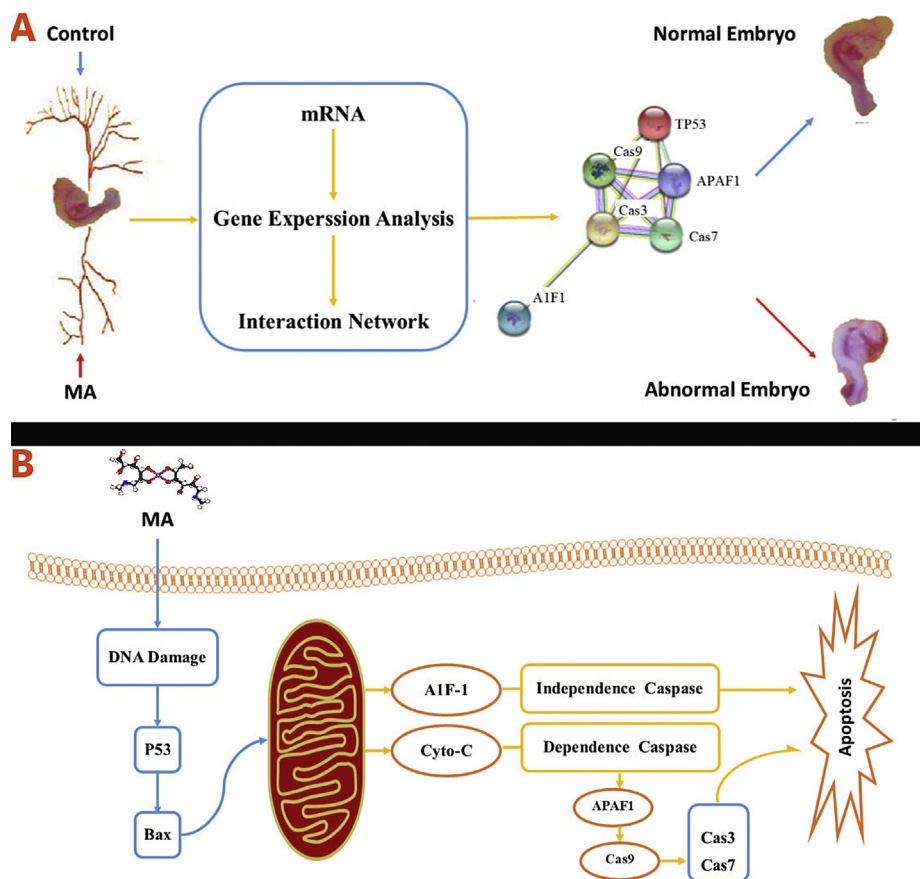


Fig. 4. (A) Gene expression analysis of meglumine antimoniate-treated embryos suggests a possible link between vascular defects, induction of apoptotic signaling pathways, altered protein-protein interaction network and early embryo malformation during pregnancy. (B) Suggested mechanism of induced vascular apoptosis by meglumine antimoniate in a chick embryo model. DNA damage can induce apoptosis through P53-dependent pathway.

in vivo chick embryo model. The chick embryo is a superior model for *in vivo* assessment of toxico-pathological effects and pharmacokinetics of drugs because of its simplicity, reproducibility of results, ethical consideration and low cost [8,18]. The chick embryo is a suitable model. Our study observed a range of outcomes and disorders related to the vascular apoptotic activity of MA in chick embryos. These outcomes are characterized below.

The first outcome was an alteration of the early vascular development in the EEM. Because of the documented decrease in vessel area and total vessel length in MA-treated embryos, it can be concluded that MA negatively affects the vascular network. This altered vascular network may provide a link between MA exposure and developmental defects such as the embryo malformation observed in the present study.

The second indication of MA disorder was the considerable alteration in the normal expression of apoptotic-regulating genes. The mechanisms and pathway by which MA-induced vascular apoptosis has not been clearly defined but based on our results, it can be concluded that the vascular apoptotic activity of MA is due to the induction of apoptotic signaling pathways. In the current investigation, the relative expression levels of CASP3, CASP7, CASP9, APAF1, AIF1 and TP53 genes increased significantly in drug-exposed EEMs.

This study lends evidence to the fact that MA at the therapeutic dosage for humans (75 mg/kg) adversely affects the embryo vasculature during the first stage of fetal growth. The severity of the lesions was highest in embryos that received the highest dosage of the drug. For example, MA at dosage of 75 mg/kg of egg weight,

fewer gross lesions were observed in the early period of embryo development, but at a dosage of 150 mg/kg, the lesions were severe and, in some instances, the embryos were thoroughly deformed.

The exact mechanism and reason for embryo malformation following MA treatment is not clearly understood, but on the explanation of the injuries to the affected embryo could be the vascular apoptotic activity of MA. This can affect the normal regulation of vessel genesis and vessel growth and lead to embryo malformation because normal intra-uterine development of the fetus is associated with the normal development of the vascular network. Moreover, the protein-protein interaction networks of evaluated genes constructed in STRING suggests that MA might alter this interaction. This effect of MA may also be involved in the alteration of vascular apoptosis, which explains the injuries and malformation in the treated embryos in our investigation. This concept requires future investigation.

We have shown that MA exposure affects the expression of apoptotic-regulating genes such as CASP3, CASP7, CASP9, APAF1, AIF1 and TP53. In addition, IHC assay has shown a low expression of BCL2 and increased expression of Bax which are associated with a high rate of apoptosis (Fig. 2B).

The expression of these genes treated with MA could be linked to the geno-toxic property of this drug, which presumably acts as a pro-mutagenic compound that causes damage to DNA [19]. DNA damage can induce apoptosis through the P53-dependent pathway. It was revealed that pro-apoptotic family members such as Bax are transcriptional targets of TP53. Following P53-induced activation of Bax, the effector phase of apoptosis begins through the release of

apoptogenic mediators from the mitochondria, including cytochrome c. This cytochrome c causes the formation of apoptosome, which consists of APAF1 and CASP9 activation following recruitment into the apoptosome. Activated CASP9 then stimulates other caspases (such as CASP3 and CASP7) which cause death. The next pro-apoptotic family member, AIF1, is also released from the mitochondria during vascular apoptosis and acts as an independent caspase [20–22]. Fig. 4B summarizes the pathway of vascular apoptosis induced by MA in a chick embryo model.

In recent years, the population of pregnant women with leishmaniasis has increased in some countries leading to an increase in their use of anti-leishmaniasis drugs [23]. Drug toxicity is of great concern during pregnancy. Meglumine antimoniate is classified as being in group C of US Food and Drug Administration (FDA) pharmacological drugs. The Insufficient investigation has been done to verify the adverse effects of this drug during pregnancy [24]. As far as the authors are aware, the current study is the first to target the vascular apoptotic effect of MA using the chick embryo model. Our results have shown that MA has adverse effects on the normal regulation of apoptotic genes and has devastating consequences (e.g. vascular defects and embryo malformation).

The data presented in this paper permit us to recommend that the administration of MA must be restricted during pregnancy or only be prescribed when benefits outweigh the risk. Consequently, the manufacture of safe alternatives should be considered as a goal.

Acknowledgements

The authors would like to thank the Leishmaniasis Research Center personnel for their help in carrying out this study. This study was financially supported by Kerman University of Medical Sciences, Kerman, Iran (project no. 94/974/205).

Transparency document

Transparency document related to this article can be found online at <https://doi.org/10.1016/j.bbrc.2018.09.152>.

References

- [1] D. Chen, J. Zheng, Regulation of placental angiogenesis, *Microcirculation* 21 (2014) 15–25.
- [2] I. Ligi, S. Simoncini, E. Tellier, I. Grandvuillemin, M. Marcelli, A. Bikfalvi, C. Buffat, F. Dignat-George, F. Anfoso, U. Simeoni, Altered angiogenesis in low birth weight individuals: a role for anti-angiogenic circulating factors, *J. Matern. Neonatal Med.* 27 (2014) 233–238.
- [3] H. Tavakkoli, A. Derakhshanfar, S. Noori Gooshki, Toxicopathological lesions of fosfomycin in embryonic model, *Eur. J. Exp. Biol.* 4 (2014) 63–71.
- [4] K. Ishihara-Hattori, P. Barrow, Review of embryo-fetal developmental toxicity studies performed for recent FDA-approved pharmaceuticals, *Reprod. Toxicol.* 64 (2016) 98–104.
- [5] W.H.O.E.C. on the C. of the L. Meeting, W.H. Organization, Control of the Leishmaniasis: Report of a Meeting of the WHO Expert Committee on the Control of Leishmaniasis, 22–26 March 2010, World Health Organization, Geneva, 2010.
- [6] A. Khosravi, I. Sharifi, H. Tavakkoli, A. Derakhshanfar, A.R. Keyhani, Z. Salari, S.S. Mosallanejad, M. Bamorovat, Embryonic toxicopathological effects of meglumine antimoniate using a chick embryo model, *PLoS One* 13 (2018), e0196424. <https://doi.org/10.1371/journal.pone.0196424>.
- [7] H. Tavakkoli, J. Tajik, M. Zeinali, Evaluating the effects of enrofloxacin on angiogenesis using the chick embryo chorioallantoic membrane model, *Iran. J. Vet. Surg.* 11 (2016) 17–22.
- [8] A. Vargas, M. Zeisser-Labouèbe, N. Lange, R. Gurny, F. Delie, The chick embryo and its chorioallantoic membrane (CAM) for the in vivo evaluation of drug delivery systems, *Adv. Drug Deliv. Rev.* 59 (2007) 1162–1176.
- [9] B.S. Kim, H. Park, S.H. Ko, W.K. Lee, H.J. Kwon, The sphingosine-1-phosphate derivative NHOBTd inhibits angiogenesis both invitro and in vivo, *Biochem. Biophys. Res. Commun.* 413 (2011) 189–193.
- [10] O. Khamessi, H. Ben Mabrouk, R. ElFessi-Magouri, R. Kharrat, RK1, the first very short peptide from *Buthus occitanus tunetanus* inhibits tumor cell migration, proliferation and angiogenesis, *Biochem. Biophys. Res. Commun.* 499 (2018) 1–7.
- [11] S.A. Mousa, M. Yalcin, P.J. Davis, Models for assessing anti-angiogenesis agents: appraisal of current techniques, in: *Anti-angiogenesis. Strateg. Cancer Ther.* Elsevier, 2017, pp. 21–38.
- [12] D. Ribatti, The chick embryo chorioallantoic membrane (CAM) assay, *Reprod. Toxicol.* 70 (2017) 97–101.
- [13] R. Morgan, J. Keen, D. Halligan, A. O'Callaghan, R. Andrew, D. Livingstone, A. Abernethie, G. Maltese, B. Walker, P. Hadoke, Species-specific regulation of angiogenesis by glucocorticoids reveals contrasting effects on inflammatory and angiogenic pathways, *PLoS One* 13 (2018), e0192746.
- [14] V. Hamburger, H.L. Hamilton, A series of normal stages in the development of the chick embryo, *J. Morphol.* 88 (1951) 49–92.
- [15] A.M. Oosterbaan, E.A.P. Steegers, N.T.C. Ursem, The effects of homocysteine and folic acid on angiogenesis and VEGF expression during chicken vascular development, *Microvasc. Res.* 83 (2012) 98–104.
- [16] A.K. Gheorghescu, B. Tywoniuk, J. Duess, N.-V. Buchete, J. Thompson, Exposure of chick embryos to cadmium changes the extra-embryonic vascular branching pattern and alters expression of VEGF-A and VEGF-R2, *Toxicol. Appl. Pharmacol.* 289 (2015) 79–88.
- [17] M.B. Vickerman, P.A. Keith, T.L. McKay, D.J. Gedeon, M. Watanabe, M. Montano, G. Karunamuni, P.K. Kaiser, J.E. Sears, Q. Ebrahim, VESGEN 2D: automated, user-interactive software for quantification and mapping of angiogenic and lymphangiogenic trees and networks, *Anat. Rec. Adv. Integr. Anat. Evol. Biol. Adv. Integr. Anat. Evol. Biol.* 292 (2009) 320–332.
- [18] R. Haselgrübler, F. Stübl, K. Essl, M. Iken, K. Schröder, J. Weghuber, Gluc-HET, a complementary chick embryo model for the characterization of antidiabetic compounds, *PLoS One* 12 (2017), e0182788.
- [19] L.F. Cantanhêde, L.P. Almeida, R.-E.P. Soares, P.V.G. Castelo Branco, S.R.F. Pereira, Soy isoflavones have antimutagenic activity on DNA damage induced by the antileishmanial Glucantime (meglumine antimoniate), *Drug Chem. Toxicol.* 38 (2015) 312–317.
- [20] M. Schuler, D.R. Green, Mechanisms of P53-dependent Apoptosis, 2001.
- [21] S. Elmore, Apoptosis: a review of programmed cell death, *Toxicol. Pathol.* 35 (2007) 495–516.
- [22] P. Strzycz, Cell death: pulling the apoptotic trigger for necrosis, *Nat. Rev. Mol. Cell Biol.* 18 (2017) 72.
- [23] E.A. Figueiro-Filho, G. Duarte, P. El-Beitune, S.M. Quintana, T.L. Maia, Visceral leishmaniasis (kala-azar) and pregnancy, *Infect. Dis. Obstet. Gynecol.* 12 (2004) 31–40.
- [24] T.F. Galvão, M.G. Pereira, M.T. Silva, Treatment of American tegumentary leishmaniasis in special populations: a summary of evidence, *Rev. Soc. Bras. Med. Trop.* 46 (2013) 669–677.